

Four-fermion Interaction Model in a Constant Magnetic Field at Finite Temperature and Chemical Potential

Tomohiro Inagaki ^{*}

*Information Media Center, Hiroshima University, Higashi-Hiroshima,
Hiroshima, 739-8521, Japan*

Daiji Kimura [†] and Tsukasa Murata [‡]

*Department of Physics, Hiroshima University, Higashi-Hiroshima,
Hiroshima, 739-8526, Japan*

February 8, 2020

Abstract

We investigate an influence of an external magnetic field on chiral symmetry breaking in a four-fermion interaction model at finite temperature and chemical potential. By using the Fock-Schwinger proper-time method, we calculate the effective potential for the four-fermion interaction model at the leading order of the $1/N_c$ expansion. A phase structure of the chiral symmetry breaking is shown on T - μ , H - T and μ - H planes. The external magnetic field modifies the phase structure. It is found that a new phase appears for a large chemical potential.

^{*}inagaki@hiroshima-u.ac.jp

[†]kimura@theo.phys.sci.hiroshima-u.ac.jp

[‡]murata@theo.phys.sci.hiroshima-u.ac.jp

1 Introduction

The strong interactions between quarks and gluons are described by QCD. In recent years much interest has been paid to the phase structure of the QCD vacuum. A chiral $SU(N)$ symmetry for quark flavors is broken down by the QCD dynamics. It is expected that the chiral symmetry is restored at high temperature and/or high density. A phase transition takes place from a hadronic matter to the quark-gluon plasma or color super-conducting phase in hot and dense objects. Such hot and dense objects are found in some cosmological objects. A phase transition of the QCD vacuum affects to the evolution of the cosmological objects.

A situation with a high temperature and density is realized at the beginning of our universe. There is a possibility that the early universe contains a large primordial magnetic field. Another dense state at low temperature is found in the core of a neutron star. Some of neutron stars are called pulsar which are dressed by a strong magnetic field and emit a high energy radiation. It was reported the existence of a magnetar which is a star with much stronger magnetic field. Therefore it is very important to investigate the thermal and magnetic effects on the QCD vacuum. To consider the dense state we introduce a chemical potential. The phase structure of the theory is studied in an external magnetic field H at finite temperature T and chemical potential μ .

At a short distance QCD has been tested in a lot of experiments by perturbative calculations. It is well established theory. However, there is no established way to treat a non-perturbative phenomena in QCD. Since a long-range correlation has an essential role to the phase transition, the QCD vacuum is determined non-perturbatively. There are many methods to deal with a non-perturbative aspect of QCD. In the present paper we consider a four-fermion interaction model as a low-energy effective theory of QCD.[1] It is known that the model has a similar feature to the non-perturbative QCD at a low energy scale. In the model a chiral symmetry is dynamically broken down through a fermion and anti-fermion condensation for a sufficiently strong four-fermion coupling.

According to the Matsubara formalism of the finite temperature field theory, a thermal effect on the chiral symmetry breaking was investigated in the Nambu-Jona-Lasinio (NJL) model.[2] For a high temperature and/or a large chemical potential the vacuum expectation value of a composite state of a fermion and an anti-fermion, $\langle\bar{\psi}\psi\rangle$, disappears and the broken chiral

symmetry is restored. A tricritical point between the first and the second order phase transition was observed in the critical curve on T - μ plane for $H = 0$. [3, 4, 5]

The procedure dealing with the external strong magnetic field was developed by Schwinger in 1951.[6] The technique is called Fock-Schwinger proper-time method. In Refs.[7, 8] the proper-time method was applied to a four-fermion interaction model to study the influence of a magnetic field on the phase structure. It is shown that an external magnetic field has an effect to practically reduce the spacetime dimensions and enhance the chiral symmetry. Thus the vacuum expectation value, $\langle\bar{\psi}\psi\rangle$, slightly increases in a magnetic field. The method is extended to variety of situations with some external fields.[9, 10, 11, 12]

Here we apply the Fock-Schwinger proper-time method to the NJL model at finite temperature and chemical potential. By using an explicit expression of a fermion propagator in an external magnetic field at finite T and μ [13], we calculate the effective potential in the leading order of the $1/N_c$ -expansion. We use the observed quantities f_π and m_π fixing the parameters in the model. The vacuum state is determined by observing the minimum of the effective potential. Evaluating it numerically, we show the phase structure of the theory on T - μ , H - T and μ - H planes and discuss a combined effects of the magnetic field, temperature and chemical potential. Finally we give some concluding remarks.

2 Effective potential with involving T , μ and H

In this section we briefly review the fermion propagator at finite T and μ with an external magnetic field and calculate the effective potential for a four-fermion interaction model in the leading order of $1/N_c$ expansion. There are some works[3, 17, 18, 14], in which the original Fock-Schwinger proper time method was applied to the finite temperature and/or chemical potential situations.[6, 15] It was pointed out that a naive Wick rotation is not always valid for a proper time integral. In order to investigate physical situations, we carefully choose the proper time contour as is shown in Ref.[13]. We apply this result to calculate the effective potential of the four-fermion interaction model.

Here we consider the NJL model which is well known as one of the low energy effective theories of QCD. The Lagrangian of the NJL model is defined by

$$\mathcal{L} = \sum_{i=u,d} \bar{\psi}_i (i\not{\partial} - Q_i \not{A}) \psi_i + \frac{G}{2N_c} \left\{ \left(\sum_{i=u,d} \bar{\psi}_i \psi_i \right)^2 + \left(\sum_{i,j=u,d} \bar{\psi}_i i\gamma_5 \vec{\tau}_{ij} \psi_j \right)^2 \right\}, \quad (1)$$

where N_c is the number of colors, the indices i, j denote the fermion flavors, Q_i is the electric charge of the quark fields, $Q_u = 2/3$, $Q_d = -1/3$ and G is the effective coupling constant. We consider two flavors of quark fields. The quark fields ψ belong to the fundamental representation of the color $SU(N)$ group and a flavor isodoublet. $\vec{\tau}$ represents the isospin Pauli matrices. This Lagrangian is invariant under a global flavor transformation and a chiral transformation. In the following calculations we omit the flavor index for simplicity. Of course all our results completely contain the contribution from the two flavors. To find a vacuum state we evaluate the effective potential for $\langle \bar{\psi}\psi \rangle$. It is more convenient to use the auxiliary field method to calculate the effective potential. Introducing the auxiliary fields σ and $\vec{\pi}$, the Lagrangian (1) reads

$$\mathcal{L} = \bar{\psi} (i\not{\partial} - Q\not{A} - \sigma - i\gamma_5 \vec{\tau} \cdot \vec{\pi}) \psi + \frac{N_c}{2G} (\sigma^2 + \vec{\pi}^2). \quad (2)$$

From the equations of motion we obtain correspondences $\sigma \sim -(G/N_c)\bar{\psi}\psi$ and $\vec{\pi} \sim -(G/N_c)\bar{\psi}i\gamma_5\vec{\tau}\psi$.

Following the standard procedure of the imaginary time formalism[16], we introduce the temperature and the chemical potential and calculate the effective potential.[5] Because of the flavor symmetry we can select the vacuum state from the degenerate ground states. Since the physical vacuum must be an isospin singlet, we set $\vec{\pi} = 0$. In the leading order of $1/N_c$ expansion the effective potential $V_{\text{eff}}(\sigma, \vec{\pi} = 0)$ is give by

$$V_{\text{eff}}(\sigma, \vec{\pi} = 0) = \frac{1}{4G}\sigma^2 - \frac{1}{2\beta V} \text{Tr} \ln \left(\frac{i\not{\partial} + Q\not{A} - i\mu\gamma_4 - \sigma}{i\not{\partial} + Q\not{A} - i\mu\gamma_4} \right), \quad (3)$$

where we assume $\mu = \mu_u = \mu_d$ and Tr denotes the trace about spacetime coordinates and spinor indices. The factor βV in the denominator comes from the 4-dimensional volume,

$$\int_0^\beta dx_4 \int_{-\infty}^\infty d^3\vec{x} = \beta V, \quad (4)$$

where $\beta = 1/(k_B T)$ with k_B the Boltzmann constant and set $k_B = 1$. The effective potential (3) is normalized to satisfy $V_{\text{eff}}(\sigma = 0) = 0$. The second term of the right-hand side of Eq.(3) is rewritten as

$$\text{Tr} \ln \left(\frac{i\cancel{\partial} + Q\cancel{A} - i\mu\gamma_4 - \sigma}{i\cancel{\partial} + Q\cancel{A} - i\mu\gamma_4} \right) = \text{Tr} \int_0^\sigma S(x, x; m) dm, \quad (5)$$

where $S(x, y; m)$ is the fermion Green function which is a solution of the Dirac equation

$$(i\cancel{\partial} + Q\cancel{A} - i\mu\gamma_4 - m) S(x, y; m) = \delta_E^4(x - y), \quad (6)$$

where $\delta_E^4(x - y) = \delta(x_4 - y_4) \delta^3(\vec{x} - \vec{y})$.

To solve the Dirac equation (6) we introduce a bispinor function $G(x, y; m)$,

$$S(x, y; m) = (i\cancel{\partial} + Q\cancel{A} - i\mu\gamma_4 + m) G(x, y; m). \quad (7)$$

Substituting Eq.(7) into Eq.(6), we get

$$\left\{ \sum_{j=1}^3 (\partial_j - iQ A_j)^2 + \frac{1}{2} Q F_{jk} \sigma^{jk} - (i\partial_4 - i\mu)^2 - m^2 \right\} G(x, y; m) = \delta_E^4(x - y), \quad (8)$$

where F_{ij} is three dimensional field strength and σ^{ij} is a half of the commutator of the gamma matrix, $\sigma_{jk} = (i/2)[\gamma_j, \gamma_k]$.

Performing the Fourier series expansion

$$G(x, y; m) = \frac{1}{\beta} \sum_{n=-\infty}^{\infty} e^{-i\omega_n(x_4 - y_4)} \tilde{G}_n(\vec{x}, \vec{y}; m) \quad , \quad \omega_n = \frac{(2n+1)\pi}{\beta} \quad (9)$$

we rewrite Eq.(8) in the form

$$\left\{ \sum_{j=1}^3 (\partial_j - iQ A_j)^2 + \frac{QH}{2} (\gamma_1 \gamma_2 - \gamma_2 \gamma_1) - (\omega_n - i\mu)^2 - m^2 \right\} \tilde{G}_n(\vec{x}, \vec{y}; m) = \delta^3(\vec{x} - \vec{y}), \quad (10)$$

where we consider the constant magnetic field along the x_3 -direction, $F_{12} = -F_{21} = H$, for simplicity. As is known, the solution of Eq.(10) is obtained by the Fock-Schwinger proper time method.[6, 15] In Ref.[14] it is pointed

out that the original Fock-Schwinger method must be modified in the case of $T \neq 0$ and $\mu \neq 0$. At finite T and μ $\tilde{G}_n(\vec{x}, \vec{y}; m)$ is determined by the proper time evolution operator $U_n(\tau)$ as

$$\tilde{G}_n(\vec{x}, \vec{y}; m) = \begin{cases} e^{-5\pi i/4} \int_{-\infty}^{-0} U_n(\vec{x}, \vec{y}; \tau) d\tau & \text{for } n \geq 0 \\ e^{5\pi i/4} \int_{+0}^{\infty} U_n(\vec{x}, \vec{y}; \tau) d\tau & \text{for } n < 0 \end{cases}, \quad (11)$$

where $U_n(\tau)$ is defined by

$$\begin{aligned} U_n(\vec{x}, \vec{y}; \tau) = & \frac{1}{(4\pi)^{3/2} |\tau|^{3/2}} \frac{QH\tau}{\sin(QH\tau)} \exp \left\{ iQ \int_{\vec{y}}^{\vec{x}} A(\xi) \cdot d\xi \right\} \\ & \times \exp \left[-\frac{i}{4} (x-y)_i QF_{ij} [\coth(QF\tau)]_{jk} (x-y)_k \right. \\ & \left. -i\tau \left\{ \frac{1}{2} QF_{jk} \sigma_{jk} - (\omega_n - i\mu)^2 - m^2 \right\} \right]. \quad (12) \end{aligned}$$

Substituting Eqs.(9) and (11) into Eq.(7), we get the fermion Green function $S(x, y; m)$. It should be noted that there is an ambiguity problem to select a proper time contour for $\mu \gtrsim T$. [17] We must carefully take the physical contour. Performing the integration about m in Eq.(5) we obtain the explicit form of the effective potential

$$\begin{aligned} V_{\text{eff}}(\sigma) = & \frac{1}{4G} \sigma^2 + \frac{e^{-3\pi i/4}}{(4\pi)^{3/2} \beta} \sum_{n=0}^{\infty} \int_{+0}^{\infty} d\tau \frac{QH}{\tau^{3/2}} \cot(QH\tau) \\ & \times e^{-i\tau(\omega_n - i\mu)^2} \left(e^{-i\tau\sigma^2} - 1 \right) + (c.c.), \quad (13) \end{aligned}$$

where $(c.c.)$ denotes the complex conjugate of the second term. At the limit $\mu \rightarrow 0$ the effective potential (13) reproduce the previous result obtained in Ref.[18]. On the other limit $T \rightarrow 0$, Eq.(13) agrees with the former works in Refs.[4, 19].

The integrand in Eq.(13) has many poles which come from $|\tau|^{-3/2}$ and $\cot(QH\tau)$ on the real axis. The contour is determined by the boundary condition to solve the Green function. The physical contour is obtained in Ref.[6] for $T = \mu = 0$. Our result must coincide with the one given by this physical contour at the limit $T \rightarrow 0$ and $\mu \rightarrow 0$. Thus, we find that the contour for the proper-time integral in the second term in Eq.(13) should be C_1 in Fig.1.

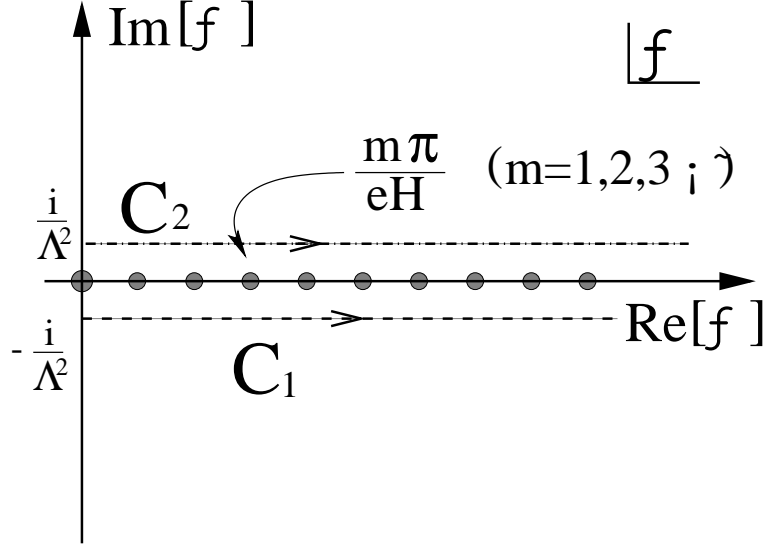


Figure 1: The contours of the integration in Eq. (13). The circles denote the poles that comes from $\tau^{-3/2}$ and $1/\sin(QH\tau)$. Λ is a proper time cut-off.

To see the contribution from the poles we rewrite Eq.(13) in the form

$$V_{\text{eff}}(\sigma) = \frac{\sigma^2}{4G} + I(\sigma) - I(\sigma = 0) + I^*(\sigma) - I^*(\sigma = 0), \quad (14)$$

where

$$I(\sigma) = \frac{e^{-3\pi i/4}}{(4\pi)^{3/2}\beta} \sum_{n=0}^{\infty} \int_{C_1} d\tau \frac{QH}{\tau^{3/2}} \cot(QH\tau) e^{-i\tau(\omega_n - i\mu)^2 - i\tau\sigma^2}. \quad (15)$$

We take the contour C_2 for the proper-time integral in $I^*(\sigma)$. After the Wick rotation on the complex τ -plane the form of $I(\sigma)$ is classified into two cases.

a) $\omega_0^2 + \sigma^2 - \mu^2 = (\pi T)^2 + \sigma^2 - \mu^2 > 0$

In this case the integrand in Eq.(15) disappears for $\tau \rightarrow -i\infty$. Hence the expression (15) can be continued to imaginary τ without encountering any

poles.

$$I(\sigma) + I^*(\sigma) = \frac{1}{4\pi^{3/2}\beta} \sum_{n=0}^{\infty} \int_{1/\Lambda^2}^{\infty} d\tau f(\sigma; n; \tau) , \quad (16)$$

$$f(\sigma; n; \tau) = \frac{QH}{\tau^{3/2}} \coth(QH\tau) \cos(2\omega_n\mu\tau) e^{-\tau(\omega_n^2 - \mu^2 + \sigma^2)} . \quad (17)$$

b) $\omega_0^2 + \sigma^2 - \mu^2 = (\pi T)^2 + \sigma^2 - \mu^2 < 0$

The integrand in (15) is exponentially suppressed at $\tau \rightarrow -i\infty$ for $n > [N]$ and at $\tau \rightarrow +i\infty$ for $n < [N]$ where $N(\sigma) = (\beta\sqrt{\mu^2 - \sigma^2}/\pi - 1)/2$ and $[N]$ is the Gauss notation. Thus we must add the residue of the poles for $n < [N]$. Thus we have

$$I(\sigma) + I^*(\sigma) = \frac{1}{4\pi^{3/2}\beta} \left[\sum_{n>[N]}^{\infty} \int_{1/\Lambda^2}^{\infty} d\tau f(\sigma; n; \tau) + \sum_{n=0}^{[N]} \left\{ h_0(\sigma; n) + h_j(\sigma; n) + \int_{1/\Lambda^2}^{\infty} d\tau g(\sigma; n; \tau) \right\} \right] , \quad (18)$$

$$g(\sigma; n; \tau) = \frac{QH}{\tau^{3/2}} \coth(QH\tau) \sin(2\omega_n\mu\tau) e^{\tau(\omega_n^2 - \mu^2 + \sigma^2)} , \quad (19)$$

$$h_0(\sigma; n) = \frac{e^{-i\pi/4}}{2} QH\Lambda \int_{-\pi/2}^{\pi/2} d\theta e^{-i\theta/2} \cot(QHe^{i\theta}\Lambda^2) \times \exp[-i\{(\omega_n - i\mu)^2 + \sigma^2\}e^{i\theta/\Lambda^2}] + (c.c.) , \quad (20)$$

$$h_j(\sigma; n) = \frac{2}{\sqrt{\pi}} \sum_{l=1}^{\infty} \left(\frac{QH}{l} \right)^{3/2} e^{-2\pi l \omega_n \mu / (QH)} \times \sin \left\{ \frac{\pi l}{QH} (\omega_n^2 - \mu^2 + \sigma^2) + \frac{3\pi}{4} \right\} . \quad (21)$$

By choosing the contour of the proper time integration carefully, we find the explicit expression for the effective potential with Eqs.(18)-(21) without any ambiguity even $\mu \gtrsim T$. This result is consistent with the previous works at the limit $H \rightarrow 0$ and $1/\Lambda^2 \rightarrow 0$. For example, the effective potential (14) exactly reproduces the result in Ref.[5] at finite T and μ .¹

¹To compare the effective potential (14) with the one in Ref.[5] we must rewrite the

3 Physical scale of G and Λ

Parameters in our model are the coupling constant G and the proper time cut-off Λ . We fix such parameters to a physical mass scale which is taken to reproduce the observed values of the pion decay constant f_π and the pion mass m_π at $T = \mu = H = 0$. Here it is assumed that T , μ and H dependence of these parameters G and Λ is not so large. We determine the values of G and Λ at $T = \mu = H = 0$ and use them at finite T , μ and H .

First we look for a relation of the proper time cut-off and the pion decay constant. The two-point function for a pion composite field is given by

$$\Gamma_\pi^{(2)}(p) = -\frac{1}{G} - \int \frac{d^4 k}{i(2\pi)^4} \int d^3 \vec{x} d^3 \vec{x}' e^{-i\vec{k}\cdot\vec{x}} e^{-i(\vec{k}+\vec{p})\cdot\vec{x}'} \times \text{tr}[(-i\gamma^5)S(\vec{x}, 0; k_0)(-i\gamma^5)S(\vec{x}', 0; k_0 + p_0)], \quad (22)$$

where $S(\vec{x}, \vec{y}; k_0)$ is a quark Green function which is defined by

$$(\gamma^0 k_0 + i\gamma^j \partial_j - \sigma)S(\vec{x}, \vec{y}; k_0) = \delta^3(\vec{x} - \vec{y}). \quad (23)$$

In this equation σ is determined by observing a stationary point of the effective potential which is a function of G and Λ . By using the proper time method $S(\vec{x}, \vec{y}; k_0)$ is written as

$$S(\vec{x}, \vec{y}; k_0) = \frac{e^{\pi i/4}}{(4\pi)^{3/2}} (i\gamma^i \partial_i + \gamma^0 k_0 + \sigma) \times \int_{-\infty}^0 \frac{d\tau}{\tau^{3/2}} \exp \left\{ -\frac{i}{4} \frac{(\vec{x} - \vec{y})^2}{\tau} + i(\sigma^2 - k_0^2)\tau \right\}, \quad (24)$$

where τ is the proper time. Substituting Eq.(24) into Eq.(22) and performing the integration about k , x and x' , we obtain

$$\Gamma_\pi^{(2)}(p) = -\frac{1}{G} + \frac{1}{4\pi^2} \int_{+0}^{\infty} d\tau ds e^{-i\sigma^2(\tau+s)} e^{ip^2\tau s/(\tau+s)} \times \frac{1}{(\tau+s)^2} \left[\frac{1}{\tau+s} \left\{ 2i - p^2 \frac{\tau s}{\tau+s} \right\} - \sigma^2 \right]. \quad (25)$$

equation by using the renormalized coupling constant G_r which is defined by the renormalization condition $\left. \frac{\partial^2 V}{\partial \sigma^2} \right|_{\sigma=\sigma_0} = \frac{1}{G_r}$

The renormalization constant for the pion wave function is defined by $\Gamma_\pi^{(2)}(p^2) = Z_\pi^{-1} p^2 + O(p^4)$. After the Wick rotation in Eq.(25) the renormalization constant Z_π is derived to be

$$Z_\pi^{-1} = \frac{1}{4\pi^2} \int_{+0}^{\infty} d\tau ds e^{-\sigma^2(\tau+s)} \frac{\tau s}{(\tau+s)^3} \left(\frac{3}{\tau+s} + \sigma^2 \right). \quad (26)$$

To obtain the relationship between f_π and Z_π we evaluate the order parameter of the chiral symmetry breaking, $[iQ_5^a, \pi^b]$, where Q_5^a is the conserved axial charge and π^a is the asymptotic pion field. By using the conserved axial current $j_\mu^a(x)$ we rewrite it,

$$\begin{aligned} \langle 0 | [iQ_5^a, \pi^b] | 0 \rangle &= \langle 0 | \left[\int d^3\vec{x} j_0^a(x), \pi^b \right] | 0 \rangle \\ &= \int d^4x i\partial^\mu \langle 0 | T j_\mu^a(x) \pi^b | 0 \rangle. \end{aligned} \quad (27)$$

The pion decay constant f_π is defined by

$$j_\mu^a(x) = f_\pi \partial_\mu \pi^a(x). \quad (28)$$

Substituting Eq.(28) into Eq.(27) we obtain

$$\langle 0 | [iQ_5^a, \pi^b] | 0 \rangle = f_\pi \delta^{ab}. \quad (29)$$

On the other hand, $j_\mu^a(x)$ and $\pi^a(x)$ are described by the quark field $\psi(x)$,

$$j_\mu^a(x) = i\bar{\psi}\gamma_\mu\gamma_5\tau^a\psi, \quad \pi^a(x) = -\frac{G}{N_c} Z_\pi^{-1/2} \bar{\psi}i\gamma_5\tau^a\psi. \quad (30)$$

Inserting Eq.(30) into the second line in Eq.(27) we get

$$\langle 0 | [iQ_5^a, \pi^b] | 0 \rangle = -\frac{G}{N_c} Z_\pi^{-1/2} \langle 0 | -2\bar{\psi}\psi | 0 \rangle \delta^{ab} = -2Z_\pi^{-1/2} \sigma \delta^{ab}. \quad (31)$$

Comparing (29) with (31), we obtain the relationship $f_\pi = -2Z_\pi^{-1/2}\sigma$. From Eq.(26) and this relationship the pion decay constant is expressed as a function of σ and Λ ,

$$f_\pi^2 = \frac{\sigma^2}{\pi^2} \int_{1/\Lambda^2}^{\infty} d\tau \left[\frac{e^{-\sigma^2\tau}}{2\tau} (1 - \sigma^2\tau) - \sigma^4\tau \text{Ei}(-\sigma^2\tau) \right], \quad (32)$$

where $\text{Ei}(-x)$ is the exponential-integral function.

As is known, pion is a massless Goldstone mode without accounting for an explicit breaking of the chiral symmetry. In QCD a small quark mass breaks the chiral symmetry. Therefore the pion field acquires a non-vanishing mass. The pion mass is obtained by the current algebra,

$$(f_\pi m_\pi)^2 = -\frac{N_c}{G} \hat{m} \langle \sigma \rangle, \quad (33)$$

where \hat{m} is the current quark mass, $2\hat{m} = m_u + m_d$. It is known as the Goldberger-Treiman relation.[20]

From the measured value, $f_\pi = 93\text{MeV}$, $m_\pi = 138\text{MeV}$ and Eqs.(32), (33) we obtain the matching condition for the coupling constant G and the proper time cut-off Λ with the physical scale. These parameters are extracted as a function of \hat{m} . Here we consider the following two cases which satisfies these matching condition.

- i) $G = 30.0\text{GeV}^{-2}$, $\Lambda = 0.953\text{GeV}$ for $\hat{m} = 5.5 \text{ MeV}$,
- ii) $G = 33.8\text{GeV}^{-2}$, $\Lambda = 0.915\text{GeV}$ for $\hat{m} = 6.0 \text{ MeV}$.

It should be noted that the phase structure on a T - μ plane dramatically changed between two cases. Evaluating the effective potential, we draw the critical line on T - μ plane in the cases, **i)** and **ii)**. In Sec.4 we give a detail of the analysis. As is shown in Fig.2, only the second order phase transition takes place in the case **i)**, while the first and the second order phase transition coexist in the case **ii)** and the tricritical point appears on the critical line. It agrees with the well-known result obtained in the other regularization procedure. In the following section we take the mass scale in the case **ii)**.

4 Phase structure

In this section we show the phase structure of the NJL model at finite T , μ and H . For this purpose we numerically calculate the effective potential (14) with $G = 33.8\text{GeV}^{-2}$ and $\Lambda = 0.915\text{GeV}$ as a function of the composite field σ .

The behavior of the effective potential is shown in Fig.3. As is seen in the figure, we observe that:

- (a) There is a second order phase transition as μ is increased with T kept

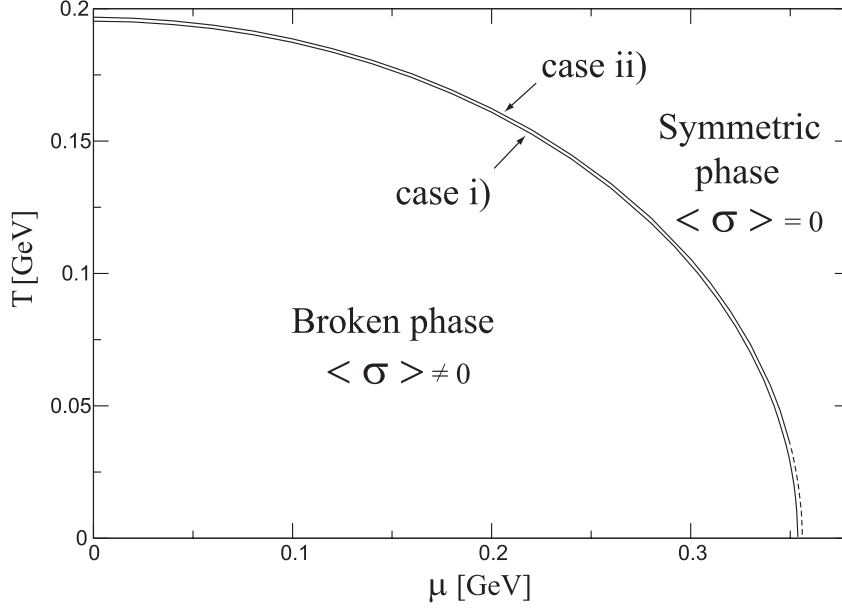


Figure 2: The critical line at $H = 0$ in the case i) and ii). The dashed line represents the first order phase transition while the solid line represents the second order phase transition.

high and H kept small.

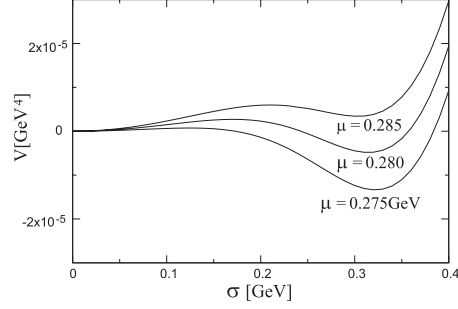
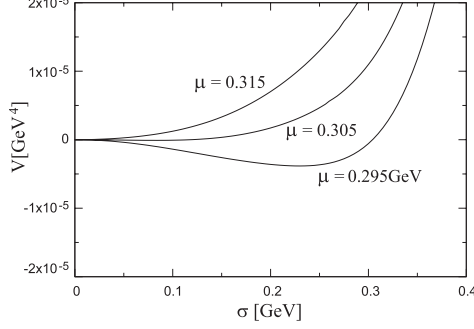
(b) There is a first order phase transition as μ is increased with H kept large and fixed.

(c) There is two steps of transitions as μ is increased with T and H kept small.

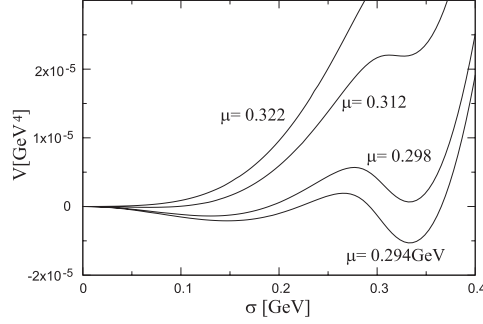
² A first order transition takes place from the third non-vanishing extremum to the first extremum. Next a second order phase transition occurs where the first non-vanishing extremum disappears.

The vacuum state is determined by observing the minimum of the effective potential. The necessary condition of the minimum is given by the gap

²Such kind of two steps transition is also found in the non-Abelian gauge theory in the Randall-Sundrum background.[21]



(a) at $T = 0.05\text{GeV}$, $H = 0.2\text{GeV}^2$ (b) at $T = 0.05\text{GeV}$, $H = 0.3\text{GeV}^2$



(c) at $T = 0.01\text{GeV}$, $H = 0.2\text{GeV}^2$

Figure 3: Behaviors of the effective potential with T , μ and H fixed.

equation

$$\left. \frac{\partial V}{\partial \sigma} \right|_{\sigma=\langle\sigma\rangle} = 0, \quad (34)$$

where $\langle\sigma\rangle$ is the vacuum expectation value of σ which corresponds to the dynamically generated fermion mass. If more than one solution exist for the gap equation (34), we numerically calculate the effective potential for each solutions and find the true vacuum expectation value $\langle\sigma\rangle$ which gives the minimum of the effective potential. In Fig.4 we plot the dynamical fermion mass $\langle\sigma\rangle$. The dynamical fermion mass disappears above a certain critical chemical potential. We clearly observe that the dynamical fermion mass

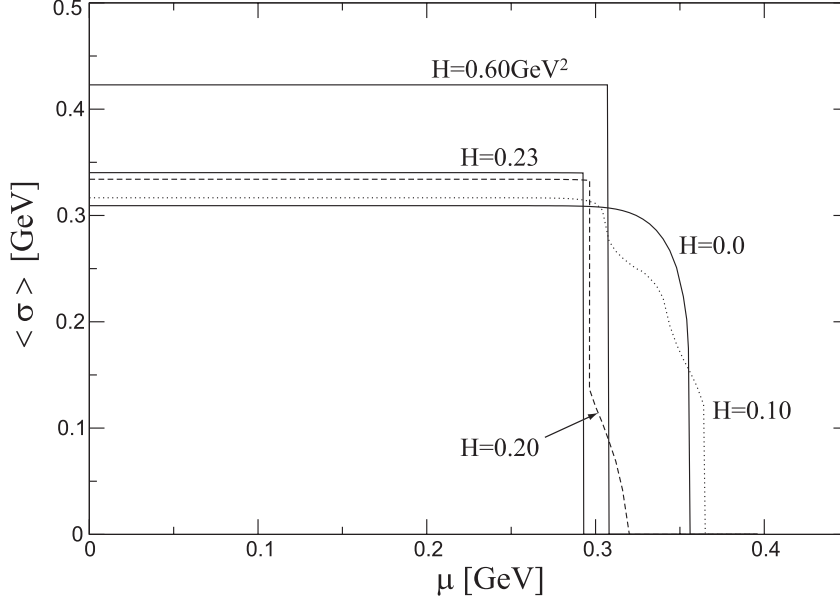


Figure 4: Dynamical fermion mass $\langle \sigma \rangle$ as a function of the chemical potential μ at $T = 0.01\text{GeV}$ with H fixed at typical values 0.0, 0.1, 0.2, 0.23 and 0.6GeV^2 .

continuously increases as H increases for a small chemical potential. The magnetic field enhances the chiral symmetry breaking. This phenomena is known as *Magnetic Catalysis*[7, 8]. For a large μ the behavior of the dynamical fermion mass has a different nature in comparison with the magnetic catalysis. Near the critical chemical potential a variety of phenomena is observed. For $H = 0.10\text{GeV}^2$ we see an oscillation of the critical line. It is called the de Haas-van Alphen effect[12, 22] which is caused when the Landau levels pass the quark Fermi surface. If H is large enough, the critical chemical potential increases as H increases and the mass gap exists at the critical μ . However we see a complex behavior of the critical chemical potential for a sufficiently small H . We clearly observe the two steps of the transition at $H = 0.20\text{GeV}^2$.

To see the situation more precisely we numerically calculate the critical value of T , μ and H where the dynamically generated fermion mass disappears. For the second order phase transition the critical point is obtained by a limit of the gap equation

$$\lim_{\langle\sigma\rangle\rightarrow 0} \left\{ \left. \frac{\partial V}{\partial \sigma} \right|_{\sigma=\langle\sigma\rangle} \right\} = 0.$$

For the first order phase transition we directly observe the behavior of the effective potential and find the critical point. Therefore we draw the phase boundary in Fig.5. On the T - μ plane it is clearly observed that the broken phase spreads out as H increased for a small chemical potential. The first order phase transition disappears near $H = 0.20\text{GeV}^2$.

We illustrate details of the phase boundary at large chemical potential on the H - T and μ - H plane. The first and second order phase transition coexist on the plane. As is seen in Fig.5(b) the broken phase is separated into two parts for $\mu \gtrsim 0.29\text{GeV}$. A distortion of the critical line at $\mu = 0.35\text{GeV}$ is caused by the de Haas-van Alphen effect. Such a effect is observed as an oscillating mode at $T = 0.01$ and 0.03GeV on the μ - H plane in Fig.5(c). In the parameter range of the second order phase transition which is described by the dashed line in Fig.5(c) the chiral symmetry breaking suppressed as H increases, while it is enhanced in the range of the first order phase transition.

5 Summary

We investigated the phase structure of the NJL model at finite temperature and chemical potential in an external magnetic field. The Fock-Schwinger proper-time method is applied to a thermal field theory in Ref.[13]. By using the two-point function obtained in Ref.[13], we calculated the effective potential which is exactly involving the effects of temperature, chemical potential and constant magnetic field in the leading order of the $1/N_c$ expansion. We showed the physical contour of the proper-time integral. There is no ambiguity for the contour of the proper-time integration for $\mu \gtrsim T$ in the expression of the effective potential.

We used the current algebra relationship with the current quark mass to determine the mass scale of the model. A place of the tricritical point strongly depends on the mass scale and the regularization procedure. In the

proper time method there is no tricritical point on the T - μ plane at $H = 0$ for the parameters determined at $\hat{m} = 5.5\text{MeV}$. Here we use the parameters determined at $\hat{m} = 6.0\text{MeV}$ where the tricritical point appears on the T - μ plane.

Through the study of the shape of the effective potential we observed the phase transition from the broken phase to the symmetric phase when the temperature T , chemical potential μ and magnetic field H vary. The temperature and chemical potential act against the chiral symmetry breaking, while the magnetic field enhance the symmetry breaking. Therefore complex behaviors of the phase boundary was emerged from the combined effects of T , μ and H , as is shown in Fig.3. We found the two steps of the transition from the broken phase to the symmetric phase for a medium size of the magnetic field, $H \sim 0.2\text{GeV}^2$. It was found that a separation of the broken phase into two parts on the $H - T$ plane. Therefore two tricritical points appeared in the critical line for $\mu \sim 0.28\text{GeV}$. More than two tricritical points were observed in the critical line at $T \sim 0.01\text{GeV}$ on the $\mu - T$ plane. In the phase diagram we saw the contributions from the magnetic field which are known as the magnetic catalysis and the de Haas-van Alphen effect.

In the present paper we regard a simple four-fermion interaction model as a low effective theory which may have some fundamental properties of the chiral symmetry breaking in QCD. Although the present work is restricted to the analysis of the phase structure of the four-fermion interaction model, we are interested in applying our result to the critical phenomena in the real world. The strength of the magnetic field which can affect the phase structure is too strong compared with the one in the core of the neutron star and the magnetar. However, an oscillating mode was observed even for a small magnetic field and may have some interesting contribution to the physics of such stars. Furthermore we expected that the magnetic field may be significantly stronger in the early stage of our universe with primordial magnetic field and contribute to the critical phenomena in the early universe.

To investigate the phenomena in dense stars we can not avoid considering the vortex configurations which generate a non-local ground state in the super-fluidity phase. It is necessary to calculate the effective action at finite μ and H . We will continue our work further and extend our analysis to a non-local ground state.

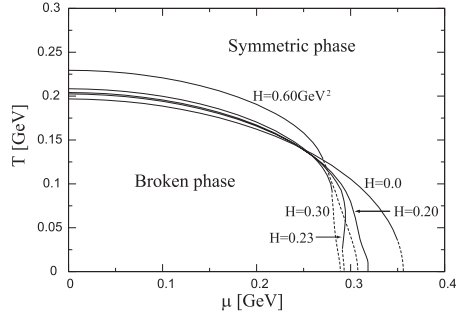
Acknowledgements

The authors would like to thank Takahiro Fujihara and Xinhe Meng for useful discussions.

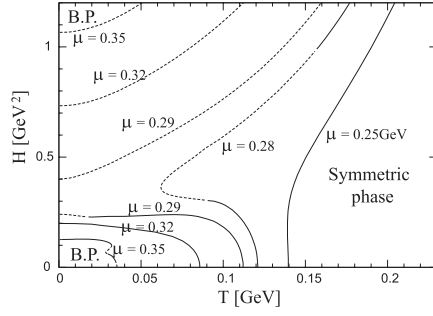
References

- [1] Y. Nambu and G. Jona-Lasinio, Phys. Rev. **124** (1961), 246.
- [2] T. Hatsuda and T. Kunihiro, KEK preprint KEK-TH 159.
V. Bernard, Ulf-G. Meissner and I. Zahed, Phys. Rev. D **36** (1987), 819.
M. Asakawa and K. Yazaki, Nucl. Phys. A **504** (1989), 668.
- [3] S. P. Klevansky, R. H. Lemmer, Phys. Rev. D **39** (1989), 3478.
H. Suganuma and T. Tatsumi, Prog. Theor. Phys. **90**(1993), 379.
M. Ishi-i, T. Kashiwa and N. Tanimura, Prog. Theor. Phys. **100** (1998), 353.
- [4] A. Chodos, K. Everding, D. A. Owen, Phys. Rev. D **42** (1990), 2881.
- [5] T. Inagaki, T. Kouno and T. Muta, Int. J. Mod. Phys. A **10** (1995), 2241.
- [6] J. Schwinger, Phys. Rev. **82** (1951), 664.
- [7] H. Suganuma and T. Tatsumi, Annals. Phys. **208** (1991), 470.
- [8] V. P. Gusynin, V. A. Miransky and I. A. Shovkovy, Phys. Rev. Lett. **73** (1994), 3499.
- [9] H. -Y. Chiu and V. Canuto, Phys. Rev. Lett. **21** (1968), 110.
H. J. Lee, V. Canuto, H. -Y. Chiu and C. Chiuderi, Phys. Rev. Lett. **23** (1969), 390.
P. Elmfors, D. Persson and B. -S. Skagerstam, Phys. Rev. Lett. **71** (1993), 480; Astropart. Phys. **2** (1994), 299.
D. Persson and V. Zeitlin, Phys. Rev. D **51** (1995), 2026.
- [10] T. Inagaki, S. D. Odintsov and Yu. I. Shil'nov, Int. J. Mod. Phys. A **14** (1999), 481.

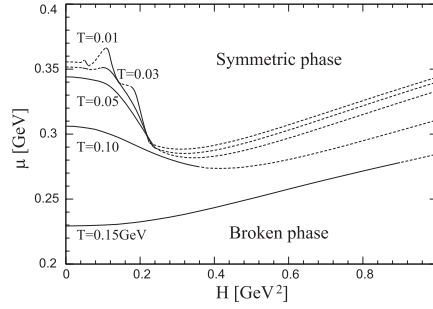
- [11] V. P. Gusynin, V. A. Miransky and I. A. Shovkovy, Phys. Rev. D **52** (1995), 4718.
S. Kanemura, H. T. Sato and H. Tochimura, Nucl. Phys. B **517** (1998), 567.
- [12] D. Ebert and A. S. Vshivtsev, hep-ph/9806421,
D. Ebert, K. G. Klimenko, M. A. Vdovichenko and A. S. Vshivtsev, Phys. Rev. D **61** (2000), 025005.
- [13] T. Inagaki, D. Kimura and T. Murata, hep-ph/0307289
- [14] P. Elmfors, Nucl. Phys. B **487** (1997), 207.
H. Gies, Phys. Rev. D **60** (1999), 105002.
J. Alexandre, Phys. Rev. D **63** (2001), 073010.
- [15] C. Itzykson and J. B. Zuber, *Quantum Field Theory* (McGraw-Hill Inc. Press, 1980)
- [16] M. Le Bellac, *Thermal Field Theory* (Cambridge University Press, 1996)
- [17] M. Haack and M. G. Schmidt, Eur. Phys. J. C **7** (1999), 149.
- [18] W. Dittrich, Phys. Rev. D **19** (1979), 2385.
- [19] D. Persson and V. Zeitlin, Phys. Rev. D **51** (1995), 2026.
- [20] T. Hatsuda and T. Kunihiro, Prog. Theor. Phys. **74** (1985), 765.
- [21] H. Abe and T. Inagaki Phys. Rev. D **66** (2002), 085001.
- [22] S. G. Sharapov, V. P. Gusynin and H. Beck, cond-mat/0308216.



(a) The T - μ plot with H fixed



(b) The H - T plot with μ fixed



(c) The μ - H plot with T fixed

Figure 5: Critical lines on T - μ plane, H - T plane and μ - H plane. The dashed line represents the first order phase transition while the solid line represents the second order phase transition.